



Contents lists available at ScienceDirect

Bioorganic & Medicinal Chemistry Letters

journal homepage: www.elsevier.com/locate/bmcl

Design, synthesis and biological evaluation of regioisomers of **666-15** as inhibitors of CREB-mediated gene transcription

Fuchun Xie^{a,1}, Bingbing X. Li^{a,1}, Xiangshu Xiao^{a,b,c,*}^a Program in Chemical Biology, Department of Physiology and Pharmacology, Oregon Health & Science University, 3181 SW Sam Jackson Park Rd, Portland, OR 97239, USA^b Knight Cancer Institute, Oregon Health & Science University, 3181 SW Sam Jackson Park Rd, Portland, OR 97239, USA^c Knight Cardiovascular Institute, Oregon Health & Science University, 3181 SW Sam Jackson Park Rd, Portland, OR 97239, USA

ARTICLE INFO

Article history:

Received 3 November 2016

Revised 28 December 2016

Accepted 28 December 2016

Available online xxx

Keywords:

CREB

Cancer

666-15

Regioisomer

Bioactive conformation

ABSTRACT

cAMP-response element binding protein (CREB) is a nuclear transcription factor that has been implicated in the pathogenesis and maintenance of various types of human cancers. Identification of small molecule inhibitors of CREB-mediated gene transcription has been pursued as a novel strategy for developing cancer therapeutics. We recently discovered a potent and cell-permeable CREB inhibitor called **666-15**. **666-15** is a bisnaphthamide and has been shown to possess efficacious anti-breast cancer activity without toxicity *in vivo*. In this study, we designed and synthesized a series of analogs of **666-15** to probe the importance of regiochemistry in naphthalene ring B. Biological evaluations of these analogs demonstrated that the substitution pattern of the alkoxy and carboxamide in naphthalene ring B is very critical for maintaining potent CREB inhibition activity, suggesting that the unique bioactive conformation accessible in **666-15** is critically important.

© 2016 Elsevier Ltd. All rights reserved.

Cancer is a heterogeneous group of complex and multigenic disease. Numerous oncogenes and tumor suppressor genes have been identified to directly contribute to the development and maintenance of transformed cellular states.¹ During the past three decades, various types of targeted therapies (e.g. kinase inhibitors and hormonal therapies) have been developed for various types of cancers.² However, most of these therapies face a formidable challenge of rapidly developed drug-resistance through up-regulating alternative cellular survival pathways.^{3,4} Therefore, identifying and targeting novel regulators of cancer development and maintenance have been the subject of intense cancer biology and chemical biology studies including those from the Cancer Genome Atlas (TCGA) project.⁵ Among these novel targets are transcription factors that are deregulated in various cancer cells.⁶

Cyclic-AMP response element (CRE) binding protein (CREB) is a stimulus-activated transcription factor.⁷ CREB normally resides in the nucleus in an inactive state.⁸ Upon phosphorylation at Ser133 by various kinases including protein kinase A (PKA), protein kinase B (PKB/Akt), p90 ribosomal S6 kinase (pp90^{RSK}) and Ras-activated mitogen activated protein kinases, CREB's transcription activity is

initiated by recruiting CREB-binding protein (CBP) and its closely related paralog p300 and other proteins in the transcription machinery to the gene promoters.^{9,10} Similar to other phosphorylated proteins, CREB phosphorylation is dynamic and tightly regulated to ensure its transcription activity is tightly coupled to the environment cues. Three protein phosphatases have been identified to be able to dephosphorylate CREB to inactivate its transcription activity. These are protein phosphatase 1 (PP1),¹¹ protein phosphatase 2A¹² and phosphatase and tensin homolog (PTEN).¹³ Mechanistically, the kinases that can phosphorylate and activate CREB are proto-oncogenes that are often overactivated in tumor cells while those phosphatases that can dephosphorylate CREB are known as tumor suppressors that are often inactivated or deleted in tumor cells. As a consequence, CREB is often overactivated in cancer cells to drive tumor development and maintenance. Indeed, this overactivation has been observed in numerous cancer tissues.^{9,14–16}

Because CREB sits at a signaling hub of multiple oncogenic signaling pathways and is overactivated in many cancer tissues, CREB has been recognized as an important oncology drug targets.⁹ We and others have been investigating small molecule inhibitors of CREB as potential cancer therapeutics.^{9,17–25} Among these, **666-15** (Fig. 1) represents the most potent inhibitor of CREB-mediated gene transcription with efficacious *in vitro* and *in vivo* anti-breast cancer activity without harming normal cellular homeostasis.^{20,26} Preliminary structure-activity relationship (SAR)

* Corresponding author at: Program in Chemical Biology, Department of Physiology and Pharmacology, Oregon Health & Science University, 3181 SW Sam Jackson Park Rd, Portland, OR 97239, USA.

E-mail address: xiaoxi@ohsu.edu (X. Xiao).

¹ These authors made equal contribution to this paper.

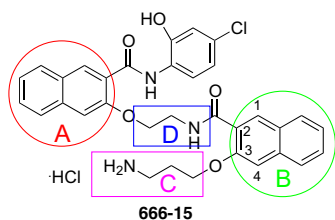


Fig. 1. Chemical structure of **666-15**.

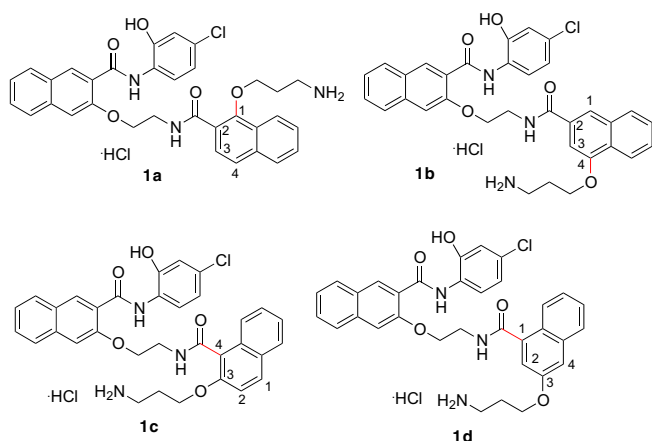
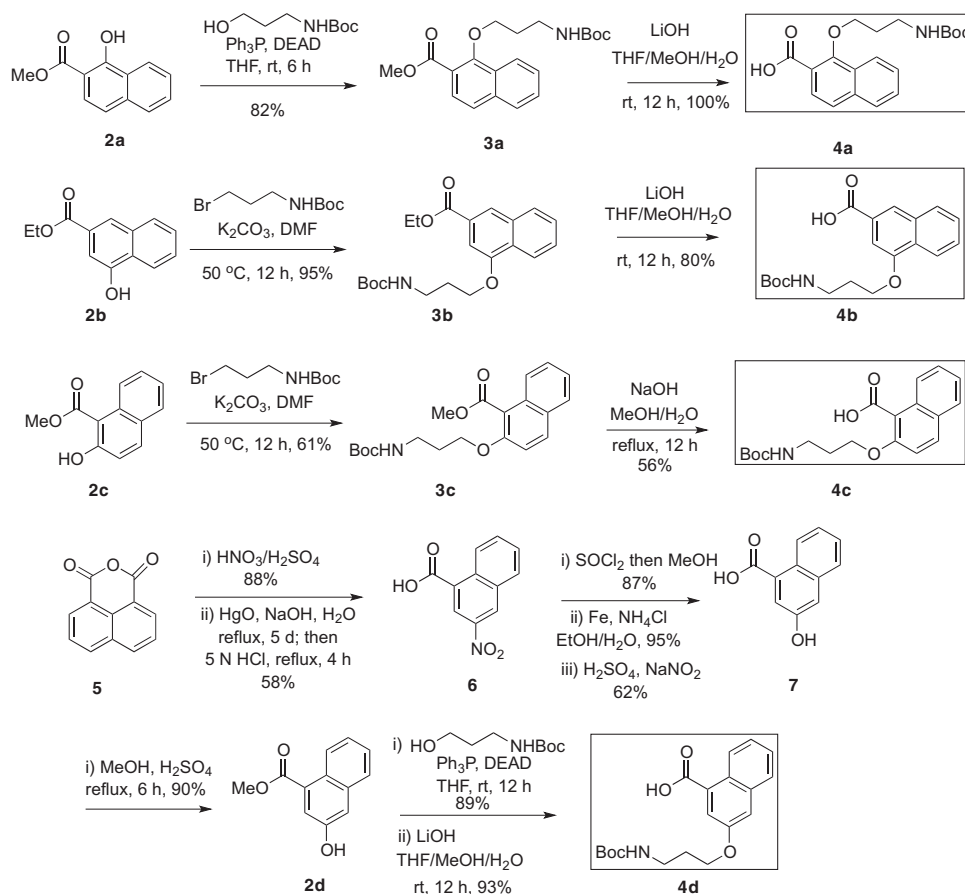


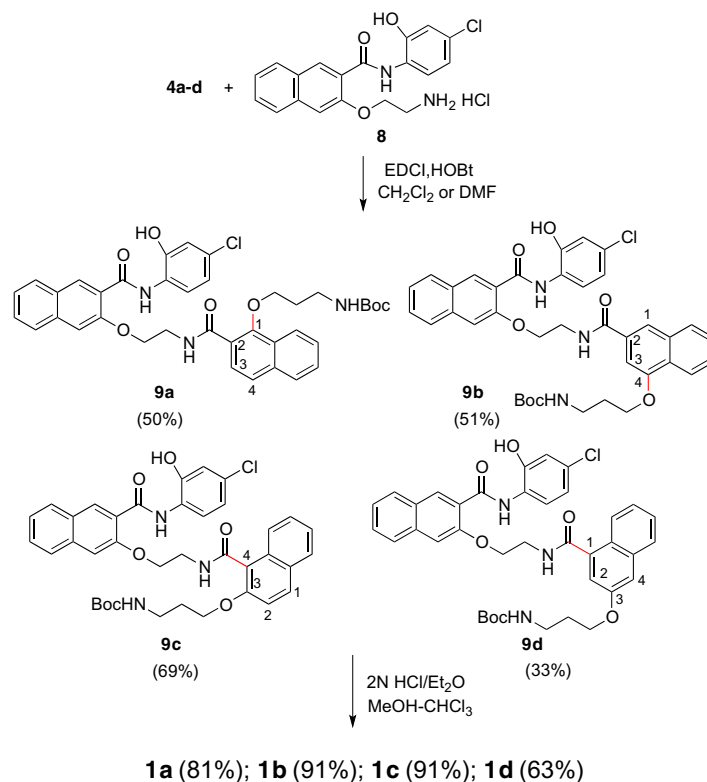
Fig. 2. Designed regioisomers **1a-1d** by changing the substitution pattern on naphthalene ring B of **666-15**.

studies identified the following (Fig. 1): (1) the naphthyl rings A and B are critical for activity; (2) minor alterations of the two carbon linkers C and D can dramatically affect the CREB inhibition activity; and (3) the primary amino group is essential for optimal CREB inhibition.²⁰ In this communication, we describe our investigation on the SAR of region B with different regioisomers by varying one substitution at a time on naphthalene ring B. By keeping the carboxamide substitution at position 2, two isomers **1a** and **1b** (Fig. 2) were designed by moving the alkoxy group to position 1 and 4, respectively. On the other hand, by maintaining the alkoxy group at position 3, isomers **1c** and **1d** (Fig. 2) were designed through changing the carboxamide substitution to position 4 and 1, respectively.

The general strategy to the synthesis of regioisomers **1a-1d** is similar to our previously described synthesis of **666-15**.²⁰ The key is to synthesize building blocks **4a-4d** (Scheme 1) and then couple them to the same amine **8** (Scheme 2). The carboxylic acids **4a-4d** were synthesized according to Scheme 1. Compounds **2a-2c** are either commercially available or could be conveniently synthesized from their corresponding acids by acid-catalyzed esterification reaction as described before.¹⁷ The Boc-protected aminopropyl side chain was either installed by Mitsunobu reaction (for **3a**) with an alcohol or *O*-alkylation reaction with a bromide (for **3b** and **3c**) to give ethers **3a-3c**, which were further saponified by LiOH or NaOH to generate required acids **4a-4c**. A more elaborate scheme to prepare **4d** was needed (Scheme 1). The acid **7** was synthesized by a reported procedure²⁷ with slight modifications. Briefly, 1,8-naphthoic anhydride was nitrated by HNO₃/H₂SO₄ followed by mercury-mediated decarboxylation of the resulting anhydride (Pesci reaction) and acidic hydrolysis to give the mono-acid **6**.



Scheme 1. Synthesis of building blocks **4a-4d**.

Scheme 2. Synthesis of regioisomers **1a-1d**.

Direct reduction of the nitro group in **6** with iron resulted in only low yield of the corresponding aniline. However, reduction of the methyl ester of **6** gave 95% yield of the corresponding aniline, which was further converted into naphthol **7** through a diazonium salt and concomitant hydrolysis of the methyl ester. The requisite building block **4d** was prepared by Mitsunobu reaction followed by saponification (Scheme 1). With all the building blocks **4a-4d** in hand, they were each coupled to amine **8**²⁰ with EDCI/HOBt as the coupling reagents to give Boc-protected amides **9a-9d** (Scheme 2). Final removal of Boc protecting group from **9a-9d** provided desired compounds **1a-1d** in good to excellent yields.²⁸

With the designed regioisomers **1a-1d** in hand, we first evaluated their potency in inhibiting CREB-mediated gene transcription in living HEK 293T cells using our previously described CREB transcription reporter assay.²⁹ This reporter assay involved transfecting HEK 293T cells with a reporter construct, which expresses *renilla* luciferase with three tandem copies of CRE sequence in the promoter region to report CREB's transcription activity in living cells. Then the transfected cells were treated with increasing concentrations of different compounds (50 nM to 50 μ M) followed by stimulation with forskolin (10 μ M) to stimulate CREB phosphorylation and transcription activity. The relative luciferase activity was used to report CREB's transcription activity. We have previously shown that **666-15** had an IC_{50} of \sim 80 nM in this transcription reporter assay.²⁰ As shown in Table 1, moving the aminopropoxy group from position 3 in **666-15** to position 1 (**1a**, IC_{50} = 23.98 ± 16.02 μ M) or 4 (**1b**, IC_{50} = 17.25 ± 3.90 μ M) resulted in significantly decreased CREB inhibition activity. Similarly, relocation of the carboxamide from position 2 in **666-15** to 4 (**1c**, IC_{50} = 18.94 ± 5.35 μ M) or 1 (**1d**, IC_{50} = 19.03 ± 10.96 μ M) also dramatically attenuated the inhibitory activity. These results show that the substitution pattern on naphthalene ring B is absolutely critical in determining the CREB inhibition activity. Previously, we have shown that **666-15** adopted a compact conformation at its global energy minimum (see also Fig. 3A).²⁰ To investigate if the regioisomers

Table 1
Biological activities of regioisomers **1a-d**.

Compd	IC_{50} (μ M) ^a	GI_{50} (μ M) ^b	
		CREB inhibition	MDA-MB-231
666-15	0.081 ± 0.04	0.073 ± 0.04	0.046 ± 0.04
1a	23.98 ± 16.02	3.12 ± 0.13	1.93 ± 0.06
1b	17.25 ± 3.90	2.68 ± 0.06	0.55 ± 0.16
1c	18.94 ± 5.35	4.31 ± 0.73	1.70 ± 0.03
1d	19.03 ± 10.96	3.82 ± 0.95	1.65 ± 0.53

^a The CREB inhibition refers to the activity of the compounds in the CREB transcription reporter assay in HEK 293T cells. The cells were transfected with a *renilla* luciferase reporter under the control of three copies of CRE. Then the cells were treated with increasing concentrations of different compounds for 30 min followed by stimulation with forskolin (10 μ M) for 6 h before luciferase measurement. The IC_{50} was calculated through non-linear regression analysis of the dose-response curves with normalized luciferase activity. The normalization was carried out through the cell lysate protein concentration in individual samples.

^b The GI_{50} was from the MTT assay after incubating the drugs with the indicated cells for 72 h. The activities of **666-15** are included for comparison purpose and are from Ref. 20.

mers **1a-1d** also adopt such a compact conformation at their global energy minimum, a conformational search was performed for compounds **1a-1d** using the same protocol as we did before.²⁰ Similar to **666-15**, the positively charged ammonium group in **1a-1d** all forms a hydrogen-bond with the carbonyl oxygen (Fig. 3B-E). The naphthalene ring B in **1a-1d** also forms π -stacking interaction with the chlorophenyl ring, effectively forming a compact conformation similar to what is observed in **666-15**. However, as the substitution pattern in the naphthalene B changes, the relative orientation of the two-carbon linker D and naphthalene ring B vary greatly compared to **666-15** (Fig. 3F). These results suggest that the unique arrangement of different groups in **666-15** forming the potential bioactive pharmacophore can not be altered without losing bioactivity.

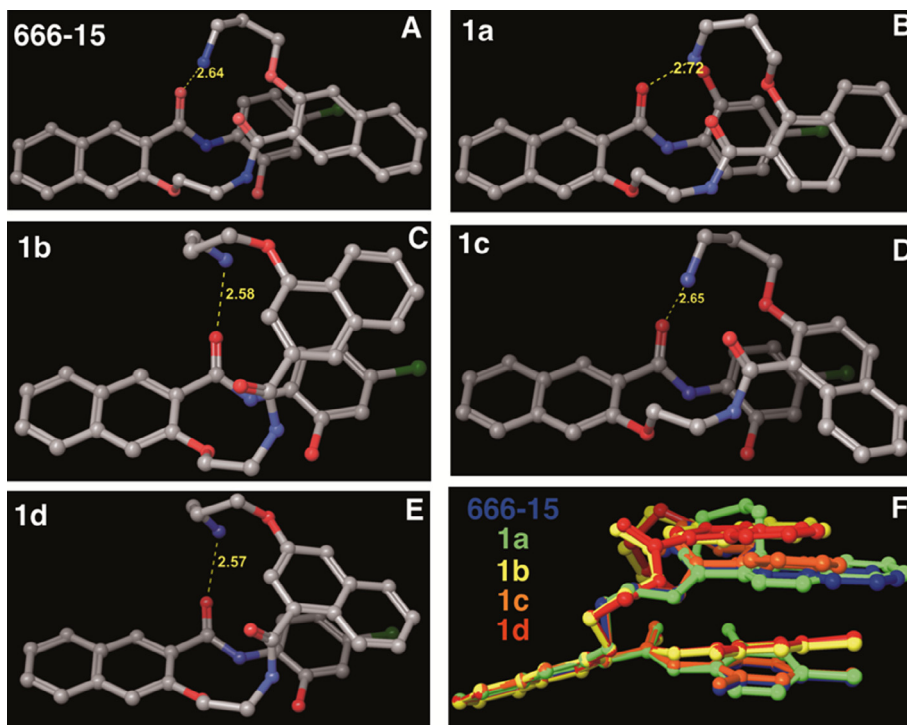


Fig. 3. Global conformational energy minima of **666-15** (A), **1a** (B), **1b** (C), **1c** (D) and **1d** (E). The yellow dotted line indicates a hydrogen bond and the corresponding interatomic distance is shown in Å. In panel (F), the conformations of **1a-1d** are superimposed onto that of **666-15**.

We also assessed the cancer cell growth inhibition activities of **1a-1d** in breast cancer MDA-MB-231 and MDA-MB-468 cells. As shown in Table 1, all four regioisomers showed significantly less potent activity than **666-15**. These results are consistent with their reduced potency in inhibiting CREB-mediated gene transcription. However, distinct difference exists for **1a-1d** between the two different assays. The growth inhibitory activity of **1a-1d** in these breast cancer cell lines is in general higher than their CREB inhibition potency. This difference suggests that **1a-1d** may be endowed with activities independent of CREB inhibition in the cells. This possibility is likely because the conformations accessible for **1a-1d** can be dramatically different from those of **666-15** due to the differential substitution pattern in naphthalene ring B.

In this study, we designed, synthesized and evaluated regioisomers of **666-15**, a potent CREB inhibitor with robust anti-breast cancer efficacy without harming normal body homeostasis. Our results showed that the alkoxy and carboxamide substitution pattern in naphthalene ring B of **666-15** is absolutely critical for maintaining potent CREB inhibition and anti-proliferative activity in breast cancer cells. These results reinforced that the unique bioactive conformation accessible only in **666-15** is the key for its potent activity. Further studies of SAR of **666-15** should keep this unique pharmacophore intact.

Acknowledgement

This work was made possible through financial supports provided by the United States National Institutes of Health (R01GM087305) and OHSU Office of Technology Transfer and Business Development.

References

1. Meacham CE, Morrison SJ. *Nature*. 2013;501:328–337.
2. Higgins MJ, Baselga J. *J Clin Invest*. 2011;121:3797–3803.
3. Lackner MR, Wilson TR, Settleman J. *Fut Oncol*. 2012;8:999–1014.

4. Riggins RB, Schrecengost RS, Guerrero MS, Bouton AH. *Cancer Lett*. 2007;256:1–24.
5. Weinstein JN, Collisson EA, Mills GB, et al. *Nat Genet*. 2013;45:1113–1120.
6. Yeh JE, Toniolo PA, Frank DA. *Curr Opin Oncol*. 2013;25:652–658.
7. Shaywitz AJ, Greenberg ME. *Annu Rev Biochem*. 1999;68:821–861.
8. Mayr B, Montminy M. *Nat Rev Mol Cell Biol*. 2001;2:599–609.
9. Xiao X, Li BX, Mitton B, Ikeda A, Sakamoto KM. *Curr Cancer Drug Targets*. 2010;10:384–391.
10. Johannessen M, Moens U. In: Caplin DE, ed. *Trends in Cellular Signaling*. Nova Publishers Inc.; 2006:41–78.
11. Hagiwara M, Alberts A, Brindle P, et al. *Cell*. 1992;70:105–113.
12. Wadzinski BE, Wheat WH, Jaspers S, et al. *Mol Cell Biol*. 1993;13:2822–2834.
13. Gu T, Zhang Z, Wang J, Guo J, Shen WH, Yin Y. *Cancer Res*. 2011;71:2821–2825.
14. Rodon L, Gonzalez-Junca A, Inda MD, Sala-Hojman A, Martinez-Saez E, Seoane J. *Cancer Discov*. 2014;4:1230–1241.
15. Zhang S, Chen L, Cui B, et al. *PLoS ONE*. 2012;7:e31127.
16. van der Sligte NE, Kampen KR, ter Elst A, et al. *Oncotarget*. 2015;6:14970–14981.
17. Jiang M, Li BX, Xie F, Delaney F, Xiao X. *J Med Chem*. 2012;55:4020–4024.
18. Li BX, Xie F, Fan Q, et al. *ACS Med Chem Lett*. 2014;5:1104–1109.
19. Li BX, Yamanaka K, Xiao X. *Bioorg Med Chem*. 2012;20:6811–6820.
20. Xie F, Li BX, Kassenbrock A, et al. *J Med Chem*. 2015;58:5075–5087.
21. Xie F, Li BX, Xiao X. *Let Org Chem*. 2013;10:380–384.
22. Xie F, Li BX, Broussard C, Xiao X. *Bioorg Med Chem Lett*. 2013;23:5371–5375.
23. Lodge JM, Rettenmaier TJ, Wells JA, Pomerantz WC, Mapp AK. *MedChemComm*. 2014;5:370–375.
24. Lee JW, Park HS, Park SA, et al. *PLoS ONE*. 2015;10:e0122628.
25. Mitton B, Chae HD, Hsu K, et al. *Leukemia*. 2016;30:2302–2311. <http://dx.doi.org/10.1038/leu.2016.1139>.
26. Li BX, Gardner R, Xue C, et al. *Sci Rep*. 2016;6:34513.
27. Duffy KJ, Darcy MG, Delorme E, et al. *J Med Chem*. 2001;44:3730–3745.
28. The characterization data are below. **1a**: a white solid, m.p. 221–222 °C. ¹H NMR (400 MHz, DMSO-*d*₆) δ 11.02 (s, 1 H), 10.52 (s, 1 H), 8.75 (t, *J* = 5.5 Hz, 1 H), 8.73 (s, 1 H), 8.43 (d, *J* = 8.5 Hz, 1 H), 8.15–8.10 (m, 1 H), 8.06 (d, *J* = 8.0 Hz, 1 H), 8.00–7.95 (m, 4 H), 7.94 (d, *J* = 8.5 Hz, 1 H), 7.74 (s, 1 H), 7.70 (d, *J* = 8.3 Hz, 1 H), 7.64–7.56 (m, 4 H), 7.46 (td, *J* = 7.5, 1.2 Hz, 1 H), 7.05 (d, *J* = 2.3 Hz, 1 H), 6.89 (dd, *J* = 8.7, 2.3 Hz, 1 H), 4.54 (t, *J* = 6.2 Hz, 1 H), 4.12 (t, *J* = 6.3 Hz, 2 H), 4.00 (q, *J* = 6.1 Hz, 2 H), 4.03 (t, *J* = 5.5 Hz, 2 H), 3.04–2.94 (m, 2 H), 2.12 (quintet, *J* = 6.9 Hz, 2 H); ¹³C NMR (100 MHz, DMSO-*d*₆) δ 167.35, 162.58, 153.63, 152.92, 148.38, 136.12, 135.61, 133.60, 129.40, 129.02, 128.46, 128.19, 128.09, 127.86, 127.53, 127.24, 126.97, 126.69, 126.31, 125.29, 124.96, 124.16, 123.01, 123.00, 121.49, 119.19, 114.93, 108.84, 73.30, 67.93, 38.91, 36.91, 28.16. **1b**: a white solid, m.p. 198–199 °C. ¹H NMR (400 MHz, DMSO-*d*₆) δ 11.03 (s, 1 H), 10.57 (s, 1 H), 8.90 (t, *J* = 5.6 Hz, 1 H), 8.74 (s, 1 H), 8.42 (d, *J* = 8.7 Hz, 1 H), 8.20–8.16 (m, 1 H), 8.05 (d, *J* = 8.2 Hz, 1 H), 8.03–7.96 (m, 4 H), 7.91 (d, *J* = 8.4 Hz, 1 H), 7.87–7.83 (m, 1 H), 7.74 (s, 1 H), 7.62–7.56 (m, 3 H), 7.45 (td, *J* = 7.5, 1.1 Hz, 1 H), 7.33 (s, 1

H), 6.97 (d, $J = 2.6$ Hz, 1 H), 6.88 (d, $J = 8.9, 2.6$ Hz, 1 H), 4.55 (t, $J = 6.3$ Hz, 2 H), 4.24 (t, $J = 5.9$ Hz, 2 H), 3.96 (q, $J = 5.5$ Hz, 2 H), 3.07 (t, $J = 6.6$ Hz, 2 H), 2.18 (quintet, $J = 6.9$ Hz, 2 H); ^{13}C NMR (100 MHz, DMSO- d_6) δ 167.31, 162.61, 154.27, 153.62, 148.28, 136.12, 133.60, 133.48, 132.47, 129.38, 129.07, 129.00, 128.17, 127.66, 127.54, 127.45, 126.92, 126.68, 126.50, 125.26, 123.05, 122.02, 121.60, 120.31, 119.26, 14.90, 108.87, 103.75, 67.86, 65.52, 38.98, 36.88, 27.35. **1c**: a white solid. m.p. 180–181 °C. ^1H NMR (400 MHz, DMSO- d_6) δ 10.99 (s, 1 H), 10.53 (s, 1 H), 8.76 (t, $J = 5.5$ Hz, 1 H), 8.74 (s, 1 H), 8.44 (d, $J = 8.4$ Hz, 1 H), 8.06 (d, $J = 8.4$ Hz, 1 H), 7.98–7.93 (m, 2 H), 7.91–7.82 (m, 4 H), 7.72 (s, 1 H), 7.67 (d, $J = 8.6$ Hz, 1 H), 7.61 (t, $J = 7.6$ Hz, 1 H), 7.49–7.43 (m, 2 H), 7.32 (t, $J = 7.5$ Hz, 1 H), 7.17 (t, $J = 7.8$ Hz, 1 H), 7.04 (d, $J = 2.3$ Hz, 1 H), 6.90 (dd, $J = 8.9, 2.3$ Hz, 1 H), 4.58 (t, $J = 5.9$ Hz, 2 H), 4.23 (t, $J = 5.9$ Hz, 2 H), 4.02 (q, $J = 5.5$ Hz, 2 H), 2.96 (q, $J = 5.9$ Hz, 2 H), 1.98 (quintet, $J = 6.5$ Hz, 2 H); ^{13}C NMR (100 MHz, DMSO- d_6) δ 167.45, 162.54, 153.75, 152.46, 148.34, 136.14, 133.63, 131.16, 130.64, 129.41, 129.02, 128.73, 128.30, 128.15, 127.44, 127.32, 127.00, 126.74, 125.26,

124.42, 124.35, 122.95, 122.33, 121.42, 119.18, 115.46, 114.90, 108.69, 67.93, 66.62, 39.02, 36.83, 27.34. **1d**: a white solid. m.p. 145–146 °C. ^1H NMR (400 MHz, DMSO- d_6) δ 11.00 (s, 1H), 10.59 (s, 1H), 8.85 (t, $J = 5.3$ Hz, 1H), 8.74 (s, 1H), 8.45 (d, $J = 8.7$ Hz, 1H), 8.11 – 8.03 (m, 2H), 8.00 (brs, 3H), 7.92 (d, $J = 8.2$ Hz, 1H), 7.81 (d, $J = 8.2$ Hz, 1H), 7.72 (s, 1H), 7.60 (t, $J = 7.5$ Hz, 1H), 7.49 – 7.42 (m, 2H), 7.39 (d, $J = 2.3$ Hz, 1H), 7.25 (t, $J = 7.6$ Hz, 1H), 7.21 (d, $J = 2.5$ Hz, 1H), 6.99 (d, $J = 2.4$ Hz, 1H), 6.90 (dd, $J = 8.7, 2.3$ Hz, 1H), 4.57 (t, $J = 5.7$ Hz, 2H), 4.15 (t, $J = 6.0$ Hz, 2H), 3.99 (q, $J = 5.3$ Hz, 2H), 2.97 (q, $J = 6.2$ Hz, 2H), 2.06 (quintet, $J = 6.0$ Hz, 2H); ^{13}C NMR (101 MHz, DMSO- d_6) δ 168.70, 162.56, 155.36, 153.78, 148.30, 136.57, 136.13, 135.02, 133.62, 129.42, 129.04, 128.14, 127.51, 127.45, 127.15, 126.90, 126.73, 125.80, 125.72, 125.24, 124.67, 122.98, 121.47, 119.22, 118.41, 114.84, 109.18, 108.68, 67.94, 65.33, 39.13, 36.73, 27.21.

29. Li BX, Xiao X. *ChemBioChem*. 2009;10:2721–2724.